Iran. J. Radiat. Res., 2008; 6 (3): 113-120

Proton beam dosimetry by CR-39 track-etched detector

M. Ghergherehchi[1, 2], H. Afarideh[1*], M. Ghanadi Maraghe[2], A. Mohammadzadeh[2], M. Esmaeilnezhad[2]

[1]Department of Nuclear Engineering and Physics, Amirkabir University of Technology, Tehran, Iran
[2]Nuclear Science and Technology Research Institute, Tehran, Iran

Background: High and intermediate energy protons are not able to form a track in a solid state nuclear track detector (SSNTD) directly. However, such tracks can be formed through secondary particles created during primary radiation nuclear reactions in a SSNTD. ***Materials and Methods:*** The protons with primary energies of 9.6 and 30 MeV available at the cyclotron accelerator with corresponding low LETs of 5.87 and 2.40 keV/µm were taken into consideration. The nuclear tracks etch rate ratio V in CR-39 were measured and transformed into LET spectra for the absorbed and equivalent dose measurements. ***Results:*** The optimum etching condition of 6 N NaOH solutions at 65 to 70 °C over a 6-hour period for the CR-39 were found initially. The corresponding bulk etching rate reached a steady rate of about 0.62 to 1.3 um/h after nine hours for an optimum etching condition. Although the LET was low, but the energy range seemed sufficient enough to create secondary particles with much higher LET through the nuclear reactions in CR-39. The relative absorbed dose contribution of the created secondary particles to the primary particles for the 9.6 and 30 MeV protons in CR-39 at 1 Gy entrance dose were 7.5 and 29.6%, respectively. ***Conclusion:*** The contribution of the secondary particle increased relatively with the proton energy decrease. This phenomenon could modify the characteristics of the energy transfer process due to secondary particles when such particles are used for radiobiological studies and/or for radiotherapy. **Iran. J. Radiat. Res., 2008; 6 (3): 113-120**

Keywords: *LET, intermediate energy protons, track etch detectors, CR-39, proton radiotherapy.*

INTRODUCTION

In order to create particle tracks, a solid state nuclear track detector (SSNTD) is exposed to nuclear radiation (neutrons or charged particles), etched, and later examined microscopically. The tracks of nuclear particles are etched faster than the bulk material and the size and shape of these tracks yield information about the mass, charge, energy, and direction of motion of the particles. The main advantages of SSNTD over other radiation detectors are the detailed information pertained in each individual particle track [(1)]. Conventional equipments, like microdosimetric tissue equivalent proportional counters, can fail in intense beams due to large predominance of low LET events. They are also limited by the defined pulses duration. Another type of detector able to establish LET of a particle are track etch detectors (TED). LET of the secondary charged particles can be established through the analysis of their track parameters [(2)]. TEDs are partially fully insensitive to low LET radiation and also to dose rates. A spectrometer of a linear energy transfer (LET) based on a chemically etched polyallyldiglycolcarbonate (commercially known as CR-39) track etched detector [(3)] employed to determine the dosimetric and microdosimetric characteristics. That is in turn relevant to the secondary high LET particles born in the detectors as a result of proton beam irradiations with primary energies of 9.6 and 30 MeV. The goal of this experiment was to study the qualitative and quantitative changes in the secondary particle characteristics with the mentioned proton energies.

**Corresponding author:*
Dr. Hossein Afarideh, Department of Nuclear Engineering and Physics, Amirkabir University of Technology, P. O. BOX: 15875-4413, Tehran, Iran.
Fax: *+98 21 66495519*
E-mail: *hafarideh@aut.ac.ir*

MATERIALS AND METHODS

Track etching system

The track detectors CR-39 available from Intercast Europe SpA via Natta 10/a 43100 Parma Italy (curing time 32 h, thickness 0.7 to 1.5 mm) were used. The small detector sheets were cut by 2 × 4 cm each. Two corners of each detector were irradiated. One corner was irradiated with ^{252}Cf fission fragments and the other corner was irradiated with ^{241}Am alpha particles. The task was done to check the exact etching conditions and to determine the bulk etching rate. After irradiation, each part of the CR-39 detector was etched in a NaOH solution as the most popular etchant which has been extensively recommended. Various concentrations from 2~10 N of NaOH solution were used at temperatures ranging from 50 to 80ºC during periods of 2 to 12 hours. After etching, the CR-39 samples were cleaned in running water for 30 minutes and dried. To determine the LET value of a particle, the etch rate ratio V ($V = V_T/V_B$; where V_B is bulk etching rate and V_T is track etching rate) was primarily established through the determination of track parameters [4]. The V-spectra obtained were corrected for the critical angle of the detection and transformed into LET spectra based on the heavy charged particles calibration curve [5]. This calibration curve from irradiations of ^{12}C to ^{56}Fe ions, with LET in water ranging from 7.9 to 200keV/µm was previously presented (figure 1). The extrapolation fitting of the data extended the calibration carves to a much higher values of LET. For secondary particles the angular distribution was related to the nuclear reaction symmetry; for slowed down primary charged particles the angular straggling at the end of the range was considered [6].

Track counting system

The etched tracks were observed using an optical microscope. The microscope image was viewed with a high-quality camera, which was connected to a home developed PC-based image analyzer. The image analyzer displays images on a monitor. The tracks appeared as dark spots on a clear white background. The recoiled particle tracks were also observed using an Atomic Force Microscope and the track parameters were measured consequently.

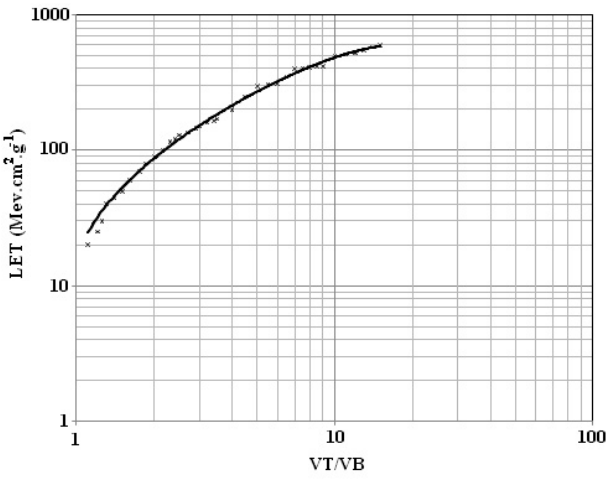

Figure 1. The obtained calibration curve from irradiations of ^{12}C to ^{56}Fe ions, with LET in water ranging from 7.9 to 200 keV/µm.

RESULTS AND DISCUSSION

Etching condition

In the search for a relatively better new etchant for CR-39 a number of new etchants have been studied. To decide whether the etchant is suitable or not, one needs to study its chemical etching properties comprehensively. Knowledge of the bulk etching rate (V_B) is useful for obtaining the true track length of any heavy ion in CR-39 detector medium. Further, the track etching rate (V_T) is the best observable quantity which provides us with a measure of the damage level. To determine V_B, V_T, and the etching efficiency (η) the Durrani and Bull (1985) procedures was employed [7].

The optimum etching condition for CR-39 used in this study turned out to be etching the CR-39 in a solution of 6 N NaOH at 66 ºC over a 6 hours period.

Figure 2 shows the changes of the bulk etching rate with normality of an aqueous solution of NaOH at 70 °C. Figure 3 shows the bulk etching rate as a function of temperature for an aqueous solution of NaOH at 6 N. It can be seen in these figures that normality has a greater effect as compared to temperature. The reproducibility of the etching temperature and normality are important because the bulk etching rate changes rapidly with temperature above 60 °C. Repeating the experiment for most of the data points confirmed that the results obtained are reproducible. The dependency of the bulk etching rate versus the etching time is shown in figure 4. It can be observed that the bulk etching rate tapers off approximately after 9 hours and it reaches to a steady rate of around 1.3 um/h with 6N NaOH at 70 °C etching condition.

LET spectra

To determine the LET value of a particle, the etching rate ratio V was primarily calculated through measurements of the track major and minor diameters viewed with a high-quality camera as presented in figure 5.

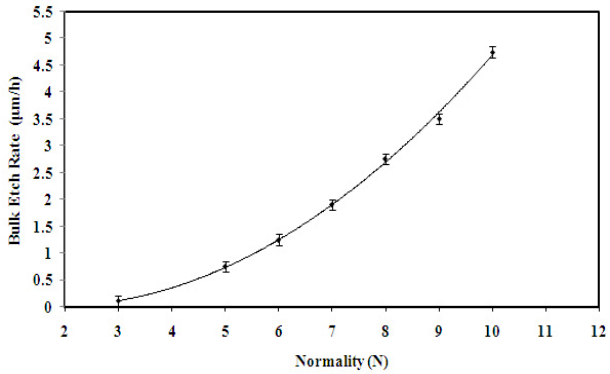

Figure 2. The bulk etching rate variation versus normality of an aqueous solution of NaOH (at Temperature: 70 °C for Time: 6h)

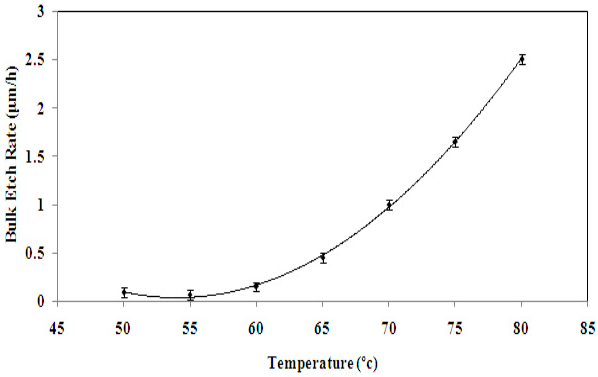

Figure 3. The bulk etching rate variation versus temperature of an aqueous solution of NaOH (at normality: 6N for Time: 6h).

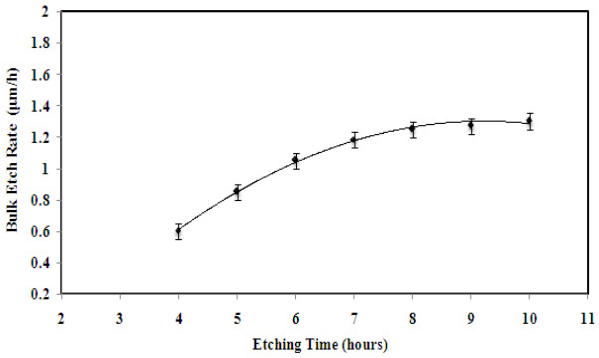

Figure 4. The bulk etching rate dependency of CR-39 versus etching time (6N NaOH at 70 °C).

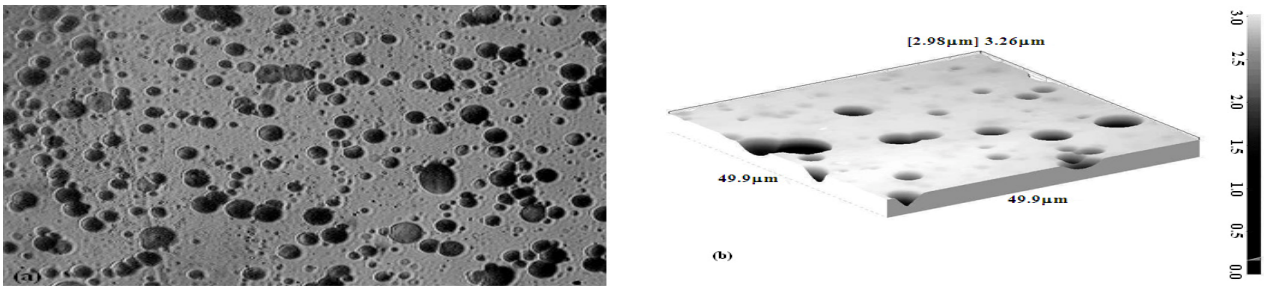

Figure 5. The typical etched tracks registered by CR-39 detector viewed by; a) optical microscope; b) atomic force microscope.

Moreover, as illustrated in figure 6, the slight deviation of the major and minor track diameters distribution from the 45° line indicates that tracks mostly have circular shapes. The spectra of V-values were collected from V > 1 up to V < 3 corresponding to 1600 > LET >178 KeV/µm in the tissue. The number of tracks in the non-irradiated (background) foils is particularly important in the region of the lowest etching rate ratios V. To minimize the importance of the background tracks, only the tracks with V > 1.1 corresponding to LET > 257 KeV/µm were taken into account. In such cases the background track densities are usually between 1 and 2000 cm^{-2}. The contributions of the particles with V > 3 to the total track number are generally low and about less than 2%. The LET spectrometer allows us to study both the dose D(L) and the dose equivalent H(L) distributions in terms of LET. For H(L) the quality factors from both recent recommendations of the International Commission on Radiological Protection (ICRP) 1990 and 2004 were used [8, 9].

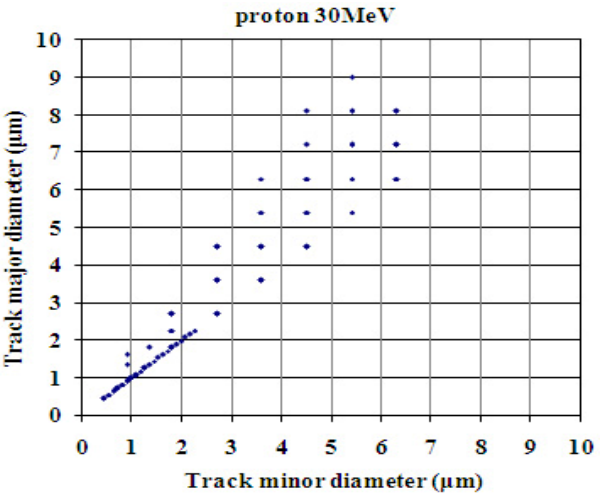

Figure 6. Major track diameters versus minor track diameters Ep =30 MeV.

The LET dose and equivalent dose distributions enable the calculation of the integral values of the dose, D, and the equivalent dose, H, corresponding to the tracks of the secondary particles which are revealed. These integral values are obtained as:

$$D = \int (\frac{dN}{dL}) L dL \qquad (1)$$

$$H = \int (\frac{dN}{dL}) L Q(L) dL \qquad (2)$$

Where dN/dL is the number of tracks in an LET interval, L is the value of the LET, and Q (L) is the quality factor corresponding to the value of L.

The calibration curve uncertainty and the statistical uncertainty are both related to the counting of tracks and contribute to the over all uncertainty. One has to consider the number of tracks and their contribution for the dose or dose equivalent in relation to the average LET in a channel. More information on particles contribution with different LET values to the total value can be obtained from the so-called micro dosimetric distributions of LN (L), LD (L) and LH (L). Such distributions for the 9.6 and 30.0 MeV protons with the event number N for the dose D as well as the equivalent dose H with ICRP 92 quality factors, H92, are presented in figures 7 to 10. It can be observed in figures 7 and 8 that with 9.6 MeV protons all three factors of LD (L), LH (L), and LN (L) insignificantly has peaked around 220 keV/µm with relatively high population of events, and they are ascending functions of LET from 260 keV/µm and beyond. The three factors of LD (L), LH (L) and LN (L) have few sporadic peaks initiated from various nuclear reactions that take place at such energy from LET of 280 to 920 keV/µm preceding the distinct broad peak from 1100 to 1400 keV/µm.

The average values of LETs with respect to the energy delivery can be estimated to about 834 keV/µm for the dose and to about 454 keV/µm MeV for the dose equivalent with ICRP 92 quality factors. The behavior of 30 MeV protons as illustrated in figures 9 and 10, LH (L), LD (L) and LN (L) were very similar in terms of

LET as in figures 7 and 8. For 30 MeV protons all three factors of insignificance peaked around 180 keV/µm with relatively high population of events and they are ascending functions of LET from 200 keV/µm and after. The three factors of LD (L), LH (L) and LN (L) have few sporadic peaks from LET of 210 to 1000 keV/µm preceding the distinct broad peak from 1100 to 1400 keV/µm. Furthermore, the average values of LETs with respect to the energy delivery can be estimated to be about 322 KeV/ µm for the dose and to be about 254 keV/µm MeV for the dose equivalent with ICRP 92 quality factors.

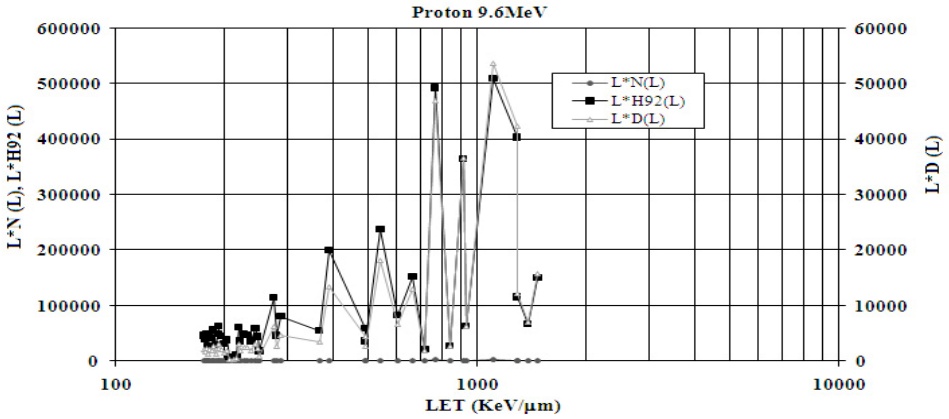

Figure 7. Event number LN(L), dose LD(L), and dose equivalent LH92(L) distributions in terms of LET for Ep = 9.6 MeV.

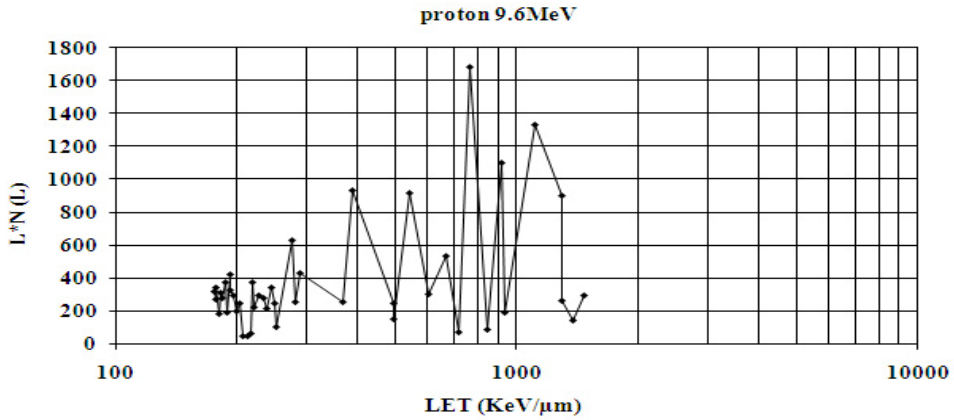

Figure 8. Event number LN (L) distribution in terms of LET for Ep = 9.6 MeV.

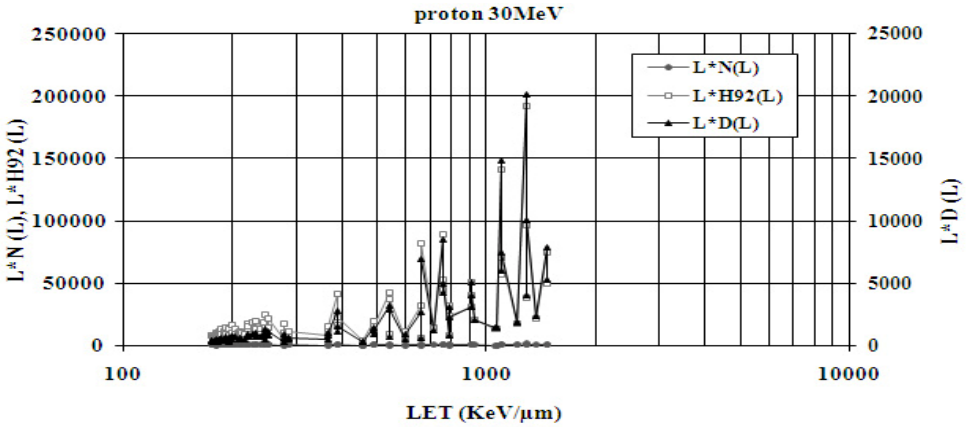

Figure 9. Event number LN(L), dose LD(L), and dose equivalent LH92(L) distributions in terms of LET for Ep =30.0 MeV.

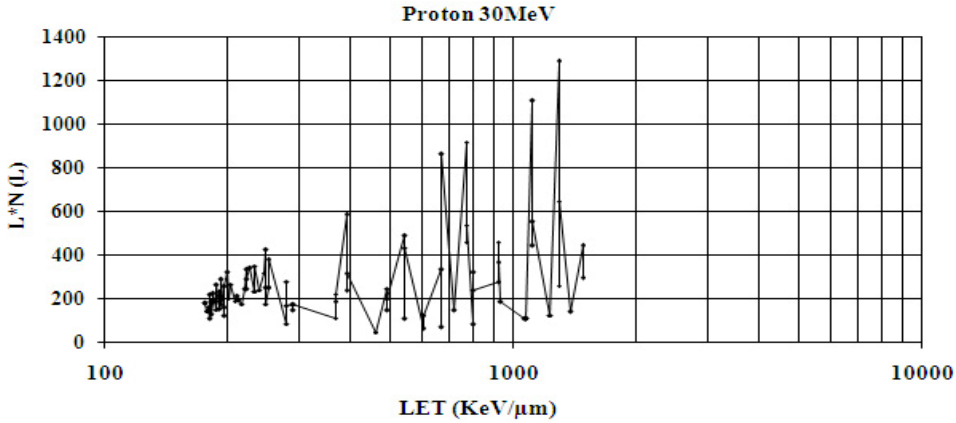

Figure 10. Event number LN (L) distribution in terms of LET for Ep = 30 MeV.

The integral characteristics of the absorbed dose D and the equivalent absorbed dose H obtained from equations (1) and (2) for the CR-39 samples which were exposed for the two beam energies are presented in table 1. It also indicates that the contribution of the secondary particles has been increasing as the proton energy decreased. Moreover, as shown in table 2, the relative absorbed dose contribution of the created secondary particles to the primary particles in CR-39 for both 1 Gy entrance dose at 30 MeV and 1 Gy entrance dose at each detector are presented.

The dose rate increased as the kinetic energy of the penetrating proton decreased with depth. The quantitative data of this increase was obtained from using STRIM code [6]; an example is presented in figure 11. Even if the dose rate increase is included in the overall dose rate, the contribution of secondary high LET particles increases and becomes evermore significant along the primary protons.

Table 1. Total dose and dose equivalents due to track forming from secondary particles created in the CR-39 LET spectrometer under intermediate energy proton irradiation for 1 Gy at 30 MeV.

Dosimetric quantity	Unit	E_P(MeV)	
		30	9.60
Absorbed dose	mGy	75.0±10.6	296.0±30.3
Dose equivalent (ICRP 92)	mSv	1245±175	4270±437
Quality factor (ICRP 92)		16.6	14.42

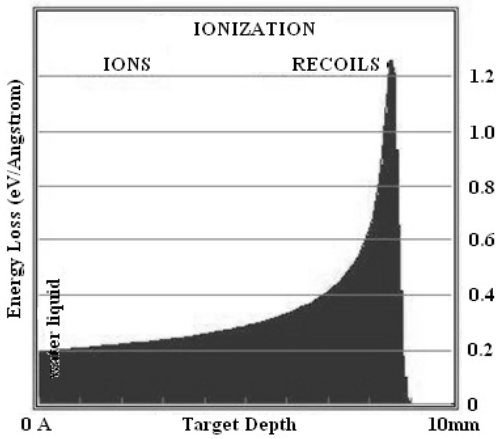

Figure 11. Depth dose distribution of the 30 MeV proton beam.

Table 2. Dose ratio of the secondary to the primary particles for 1 Gy entrance dose for different proton energies.

E_p(MeV)	Dose ratio of the secondary to the primary particles for 1 Gy entrance dose at each detector	Dose ratio of the secondary to the primary particles for 1 Gy entrance dose at 30 MeV
30	7.5	7.5
9.60	11.8	29.6

CONCLUSION

The results proved that the contribution of high LET secondary particles to the dose characteristics for 9.6 and 30.0 MeV proton energies were more significant as compared to their contribution at higher proton energies [10]. This phenomenon could be imperative in such fields as radiotherapy, radiobiology, and radiation protection. As far as proton radiotherapy and proton radiobiology studies are concerned, the dose due to secondary high LET charged particles changes not only quantitative, but also qualitative characteristics of the beam. Since the contribution of the secondary charged particles to the absorbed dose at the beam entrance at 9.6 and 30.0 MeV energies were more significant, the absorbed dose would increase substantially at greater depths. Besides, due to the increased percentage of high LET particles, radiobiological characteristics of the beam may also change with the depth.

REFERENCES

1. Cassou RM and Benton EV (1978) Properties and applications of CR-39 polymeric nuclear track detector. *Nuclear Track Detection,* ***2****: 173- 179.*
2. Fleischer RL, Price PB, Walker RM (1975) Nuclear tracks in solids. University of California Press, Berkeley, USA.
3. Spurn'y F, Bedn'ar J, Turek K (1997) Spectrometry of linear energy transfer with a track etch detector. *Radiation Measurement,* ***28****: 515–518.*
4. Nikezic D and Yu KN (2004) Formation and growth of tracks in nuclear track materials. *Materials Science and Engineering R,* ***46****: 51–123.*
5. Spurny F, Jadrnickova I, Bamblevski VP, Molokanov AG (2005) Upgrading of LET track-etch spectrometer calibration: Calibration and uncertainty analysis. *Radiation Measurement,* ***40****: 343- 346.*
6. Ziegler JF, Biersack P, Littmark U (1986) in: Ziegler JF (Ed.) The stopping and range of ions in matter. Pergamon Press, New York, USA.
7. Durrani SA and Bull RK (1987) Solid state nuclear track detection. Pergamon Press, Oxford, UK.
8. ICRP (2004) Recommendations of the international commission on radiological protection: Relative biological effectiveness (RBE), Quality factor (Q), and radiation Weighting factor (WR). *ICRP Publication,* ***92:*** *9 - 12.*
9. ICRP (1990) Recommendations of the international commission on radiological protection. *ICRP Publication 60, Annals of ICRP,* ***21:*** *1–3.*
10. Spurn'y F, Bamblevski VP, Molokanov AG, Vlcek B (2001) Dosimetric and microdosimetric characteristics of high energy proton beams. *Radiation Measurement,* ***34****: 527- 531.*